Impact of anthropized river hydrodynamic conditions on the downstream migration of Atlantic salmon smolts

Authors:

Utashi D. Ciraane[1], Damien Sonny[2], Marc Lerquet[2], Pierre Archambeau[1], Benjamin Dewals[1], Michel Pirotton[1], Pierre Sacré[3], Jean-Philippe Benitez[4], Michaël Ovidio[4], Sébastien Erpicum[1]

[1]*UR-UEE, Laboratory of Hydraulics in environmental and civil engineering (HECE), University of Liège, Belgium*

[2]*PROFISH, Belgium*

[3]*Department of Electrical Engineering and Computer Science, University of Liège, Liège, Belgium.*

[4]*UR-FOCUS, Management of Aquatic Resources and Aquaculture Unit (UGEAA), University of Liège, Liège, Belgium*

Abstract

Knowledge gaps persist regarding the influence of river hydrodynamics (e.g., flow velocity, depth, temperature, pressure) on the seaward migration of young Atlantic salmon (smolts). These gaps are reflected in rivers by the reduction of safe migration routes for salmons caused by the artificial flow alteration from hydraulic structures such as dams. The situation has long contributed to the disappearance of Atlantic salmon in many rivers and hinders their sustainable reintroduction. To better understand the hydrodynamic factors influencing smolt migration speeds, this study examines the downstream migrations of 491 hatchery smolts over three years (2017, 2021, and 2023) characterized by contrasting hydrological conditions and distinct flow patterns. The study covers 82 km of the Meuse River in Belgium, where smolts crossed six reaches delimited by movable weirs. Smolt trajectories were tracked using acoustic telemetry from 12 detection sites. A one-dimensional hydrodynamic model calculated the water velocities encountered by smolts, while water temperature and the diurnal

pattern were also monitored. The results confirm the positive correlation between flow velocities and smolt migration speeds suggested in the literature. Flow velocities below one body length per second (approximately 0.15 m/s) disorient smolts. However, smolts slowed at relatively high velocities, as shown by the negative correlation between flow velocities and relative migration speeds. Additionally, migration speed increased with distance travelled and daytime but decreased with water temperature. These findings pave the way for the implementation of more science-based environmental flow conditions in human-altered rivers during the migration season of smolts.

Keywords: Atlantic salmon, Smolt, Migration, Velocity, Hydrodynamic, Etho-hydraulic, Ecohydraulics.

1. Introduction

Dams distort river hydrodynamics and ecosystems. Generally, dams are built to control river flows. They enable droughts and floods management, drinking water storage, production of renewable electricity, irrigation, fluvial transportation, recreative activities (Tortajada, 2015; Chen et al., 2016; Lucas-Borja et al., 2021). However, by creating novel and artificial flow conditions, these infrastructures alter upstream and downstream rivers hydrodynamic and ecology (Grill et al., 2019). Dams limit aquatic life movements and habitats, reduce nutrients and sediments transport, alter water quality and temperatures (Pompeu et al., 2022; Wang et al., 2022; Chen et al., 2023). Although the impacts of dams on river hydrodynamics are relatively well known and controlled, the understanding of the impacts of flow conditions on aquatic life movements remains limited (Silva et al., 2018; Franklin et al., 2024). Knowledge gaps persist on how aquatic species are affected by hydrodynamic conditions (water velocity, depth, temperature, spatial and temporal velocity gradients, pressure) throughout their life stages. To sustain global aquatic biodiversity, it is essential to enhance our understanding of the relationship between hydrodynamic conditions and behaviours of aquatic species. Addressing this challenge demands significant efforts but its outcomes will facilitate the adaptation of human-altered river flows to meet the needs of aquatic fauna, especially migratory species.

The Atlantic salmon (*Salmo Salar*) exemplifies this challenge. During the smolt phase, juvenile salmons (smolts) migrate downstream from freshwater to the ocean. Smolts mature in the ocean before returning to rivers for spawning (Thorstad et al., 2021). However, the limited understanding of the relationship between river hydrodynamics and salmon migrations favoured the construction of multiple migration obstacles in rivers which led to the disappearance of safe upstream and downstream migration routes for salmon in many human-altered rivers. The phenomenon contributed to the decline in salmon populations in many river basins (Van Rijssel et al., 2024). Today, solutions have been proposed to restore safe migration routes near obstacles for Atlantic salmon in anthropized rivers (Scruton et al., 2003; Fjeldstad et al., 2012; Bunt et al., 2012; Szabo-Meszaros et al., 2019; Watson et al., 2022; Peirson & Harris, 2025). Nevertheless, most solutions struggle with attractiveness and effectiveness (Bunt et al., 2012; Renardy et al., 2023a). Atlantic salmons often have difficulties locating human-made migration routes, and the effectiveness of these solutions varies significantly with time and location (Ben Jebria et al., 2023; Renardy et al., 2023 a). For seaward migrations, the primary challenge lies in guiding smolts towards safe migration routes under all flow conditions. Addressing this challenge requires a thorough understanding of the environmental cues used by smolts during their seaward migration along the river (Gibeau et al., 2017).

A non-systematic review of the recent literature suggests that flow conditions and the diel pattern are key factors in the downstream migration of juvenile Atlantic salmons (**Table 1**). The review aimed to identify and understand the main environmental cues used by smolts during their seaward migration. Keywords for the search included environmental cues, downstream migration, smolts, Atlantic salmon, telemetry, and river. Among the 82 papers identified, the non-systematic review primarily concentrated on recent studies conducted in rivers. Laboratory studies were generally excluded to minimise potential environmental biases introduced by the artificial nature of laboratory setups, such as scale effects, flume materials, and measurement devices.

Table 1: Non-systematic review of the impacts of flow hydrodynamics and nychthemeral cycle on the downstream migration of Atlantic salmon smolts.

	Davidsen et al. (2005)	Dolotov (2006)	Ibbotson et al. (2006)	Roberts et al. (2009)	Fjeldstad et al. (2012)	Martin et al. (2012)	Riley et al. (2012)	Thorstad et al. (2012)	Otero et al. (2014)	Zydlewski et al. (2014)	Aldvén et al. (2015)	Havn et al. (2018)	Strople et al. (2018)	Szabo-Meszaros et al. (2019)	Harvey et al. (2020)	Silva et al. (2020)	Teichert et al. (2020)	Bjerck et al. (2021)	Honkanen et al. (2021)	Ovidio et al. (2021)	Renardy et al. (2021)	Simmons et al. (2021)	Vollset et al. (2021)	Erpicum et al. (2022)	Lilly et al. (2022)	Ben Jebria et al. (2023)	Doogan et al. (2023)	Renardy et al. (2023 a)	Renardy et al. (2023 b)	Sortland et al. (2024)
Smolts use the flow as a migration cue.	✓				✓		✓	✓	✓		✓	✓		✓	✓	✓	✓	✓	✓	✓	✓	✓		✓	✓	✓	✓	✓	✓	✓
Low velocities disorient smolts.																			✓		✓				✓	✓				
. Smolts follow high (main) flow velocity.								✓						✓		✓					✓	✓			✓	✓	✓	✓	✓	✓
High velocities slow down smolts.								✓																						✓
Water temperatures affect smolts migration.		✓			✓	✓		✓	✓	✓			✓		✓		✓					✓	✓							
Water temperatures trigger smolts migration.								✓	✓	✓					✓		✓													
Water temperatures affect smolts swimming speed.		✓				✓		✓	✓				✓									✓								
Water temperatures stop smolts migration.						✓																								
Smolts migrate at night.			✓	✓				✓			✓									✓										✓
Smolts migrate day and night at end of the migration season.			✓					✓			✓											✓					✓			✓
Smolt migrate during daytime for high water temperatures.			✓					✓																						
The diel pattern impacts the smoltification process.					✓					✓																				

The migration window of smolts is characterized by changes in river hydrodynamics, particularly river discharges and temperatures (Harvey et al., 2020; Teichert et al., 2020; Bjerck et al., 2021). Being an aggregate value, discharge variations induce changes in water velocities and/or water depths in a given river section (Gore & Banning, 2017). Up to now, the literature has mainly explored the impact of flow velocities due to significant variability of water depths within and between rivers. Moreover, as noticed by Thorstad et al. (2012), it was formerly believed that smolts drifted passively with the flow. However, recent studies show that smolts actively swim in rivers (Davidsen et al., 2005; Thorstad et al., 2012;

Silva et al., 2020; Ben Jebria et al., 2023; Renardy et al., 2023 b). This is evidenced by smolt swimming speeds, which can exceed or fall below flow velocities and by smolt explorations of multiple migratory routes near obstacles. Nonetheless, the literature emphasizes that smolts follow the main flow, even though, only a few studies have proposed velocities threshold for guiding juvenile salmons downstream.

Low water velocities disorient smolts and the intensity of flow velocity is crucial for guiding smolts towards the sea. Upstream movements of smolts are typically observed at flow velocities below 0.15 m/s (Renardy et al., 2021). Additionally, studies in standing water bodies such as natural lakes show that smolt trajectories frequently deviate from the outlet with sometimes up to 49% of trajectories in the opposite direction of the seaward migration (Honkanen et al., 2021; Lilly et al., 2022). The migration speed is also slow in standing waters (Lilly et al., 2022). Near obstacles, smolts struggle to find migration routes when flow velocities at route entrances are below 0.2 m/s (Ben Jebria et al., 2023; Renardy et al., 2023 b). Thus, smolts have a flow velocity threshold above which the seaward direction is clear.

In contrast, high water velocities favour rapid migration of smolts. Although no upper velocity limit tolerable by smolts has been proposed, the downstream migration speeds generally increase with high flow velocities (Renardy et al., 2023 a; b). The number of smolts migrating downstream also increases with high velocities generated by peak flows during the migration season (Teichert et al., 2020; Bjerck et al., 2021). However, laboratory studies on both Atlantic and Chinook salmons suggested that smolts exhibit positive rheotaxis and avoidance behaviours in response to strong and abrupt changes in the flow velocity (Enders et al., 2009; Erpicum et al., 2022). Swimming head against the current allows smolts to better control their movements in the flow and thus protect themselves from potential dangers (Thorstad et al., 2012).

Temperature influences the migration window of smolts (Vollset et al., 2021). Smolts migrate when the water temperature is above 7°C, even though subtle differences exist between regions (Harvey et al., 2020; Teichert et al., 2020). Consequently, they migrate downstream generally in spring (Whalen et al.,

1999; Jutila & Jokikokko, 2008; Thorstad et al., 2012). Thorstad et al. (2012) observed that the survival rate of post-smolts improves when smolts enter the sea at temperatures ranging from 8 to 12°C, with variations depending on rivers. Similarly, the maximal swimming speed of hatchery reared smolts is observed when the water temperature is around 10.5°C (Martin et al., 2012). Smolts also decrease their swimming speeds by 80% at temperatures below 4°C and above 17°C (Dolotov, 2006; Martin et al., 2012). Hatchery smolts may halt their migration when the water temperature exceeds 20°C (Martin et al., 2012).

Early in the migration season, smolts movements are mostly nocturnal (Hvidsten et al., 1995; Roberts et al., 2009; Ovidio et al., 2021). Night releases promote nocturnal migration for hatchery reared salmon (Roberts et al., 2009). Towards the end of the migration window, characterized by high temperatures (> 12°C) and proximity to the sea, smolts migrate both day and night (Ibbotson et al., 2006; Fjeldstad et al., 2012; Sortland et al., 2024). This shift between nocturnal and diurnal locomotion is linked to smolt strategy to either avoid predators or maximize feeding (Roberts et al., 2009). Thus, smolts migrate day and night but with a preference for nighttime.

Among the environmental variables suggested by the literature, the flow velocity plays a major role in the seaward migration of smolts. By causing upstream movements or by accelerating the migration, the flow velocity guides juvenile salmons towards the sea while affecting their migration speeds. Thus, it is crucial to improve our understanding of the links between flow velocities and smolts migration speeds in rivers. This study contributes to that goal by comparing data from smolt trajectories with flow conditions obtained from numerical hydraulic models. The objective was to examine the effect of flow velocities on smolt migration speeds. Smolts data were gathered along 82 km of an anthropized river where hatchery smolts were tracked over three years characterized by distinct hydrological conditions. The effects of water temperature and the diel pattern were also investigated for a holistic view of the seaward migration speeds.

2. Methodology

2.1. Case study

This study focuses on 82 km of the Meuse River in Belgium. The Meuse River is a 925 km long transboundary river with a catchment of 36,000 km². The Meuse River sources in France at Pouilly-en-Bassigny and flows through Belgium and The Netherlands as depicted in **Figure 1**. The river discharges its waters in the North Sea via the Rhine-Meuse-Scheldt delta. The 82 km section of the mid-lower Meuse River investigated by this study is in Belgium between the bridge of Jambes in Namur and the dam of Lixhe near the border with The Netherlands as shown in **Figure 1**.

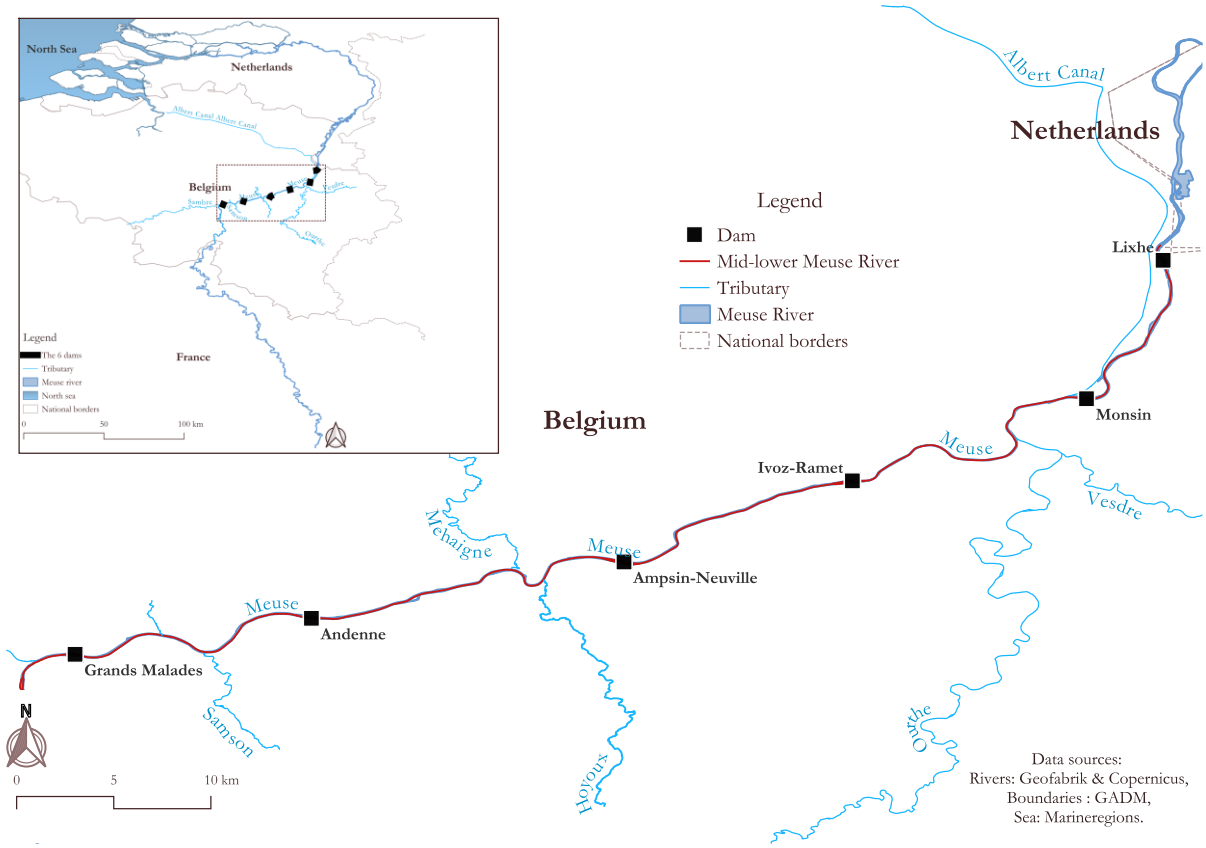

Figure 1: The mid-lower Meuse River and its major tributaries in Belgium.

The mid-lower Meuse River is fragmented by anthropogenic infrastructures. In the case study, the river features six movable weirs (low head dams) and one navigation canal, as shown in **Figure 1**. The six dams regulate water levels for navigation. They also create the hydraulic heads used to produce run-

144 of-the-river hydroelectricity. These hydraulic facilities typically include a movable dam, navigation locks,
145 and a hydroelectric power plant (HPP). The last two dams downstream (Monsin and Lixhe) lack
146 navigation locks directly at the dam site since these navigation infrastructures are located at other
147 places between the Albert Canal and the Meuse River reach.

148 The Meuse River includes over 36 fish species. The main taxa are Cypriniformes, Perciformes,
149 Salmoniformes, and Anguilliformes (Philippart, 2008; Benitez et al., 2022). At the end of the 19th
150 century, the Atlantic salmon was still abundant in the Meuse River (Prignon et al., 1999). However, a
151 significant decline in salmon populations was observed from the 1930s, probably related to numerous
152 dams and the anthropogenic alterations of the river. Since 1987, considerable efforts have been made
153 to reintroduce the Atlantic salmon into the Meuse River and its tributaries (Philippart et al., 1994;
154 Life4Fish, 2023; Benitez et al., 2024). Today, the returns of a few adult Atlantic salmons are reported
155 and monitored in the watershed. Fish ladders continue to be installed and improved for adults, but the
156 downstream migration of smolts remains challenging, despite the recent attempts of improvement
157 (Ben Ammar et al., 2020; Renardy et al., 2021; Life4Fish, 2023; Ovidio et al.2023).

158 ### 2.2. Smolt trajectory data

159 The smolt data used in this study were obtained by PROFISH company during the European project
160 LIFE4FISH (2017-2023). The LIFE4FISH project aimed at validating and implementing protective
161 measures for the downstream migration of young Atlantic salmon (smolts) and eels in the mid-lower
162 Meuse River in Belgium (Ben Ammar et al., 2020; Erpicum et al., 2022; Life4Fish, 2023). Over three
163 years (2017, 2021 and 2023), the project monitored the downstream migration of 584 young Atlantic
164 salmons using acoustic telemetry along the 82 km of the case study, as shown in **Figure 2**. The smolts
165 tagged and released in the Meuse River were 146 in 2017, 237 in 2021, and 201 in 2023. Among these
166 smolts, 491 were detected by the tracking system as shown in **Figure 2**. The monitored individuals were
167 hatchery-reared smolts from the Erezée hatchery in Belgium. Although differences exist between the
168 behaviours of wild and hatchery-reared salmons as noticed by Jonsson et al. (1991) & Nilsen et al.

(2023), hatchery-reared smolts were used due to the small and fragile salmon population in the Meuse River (Renardy et al., 2021).

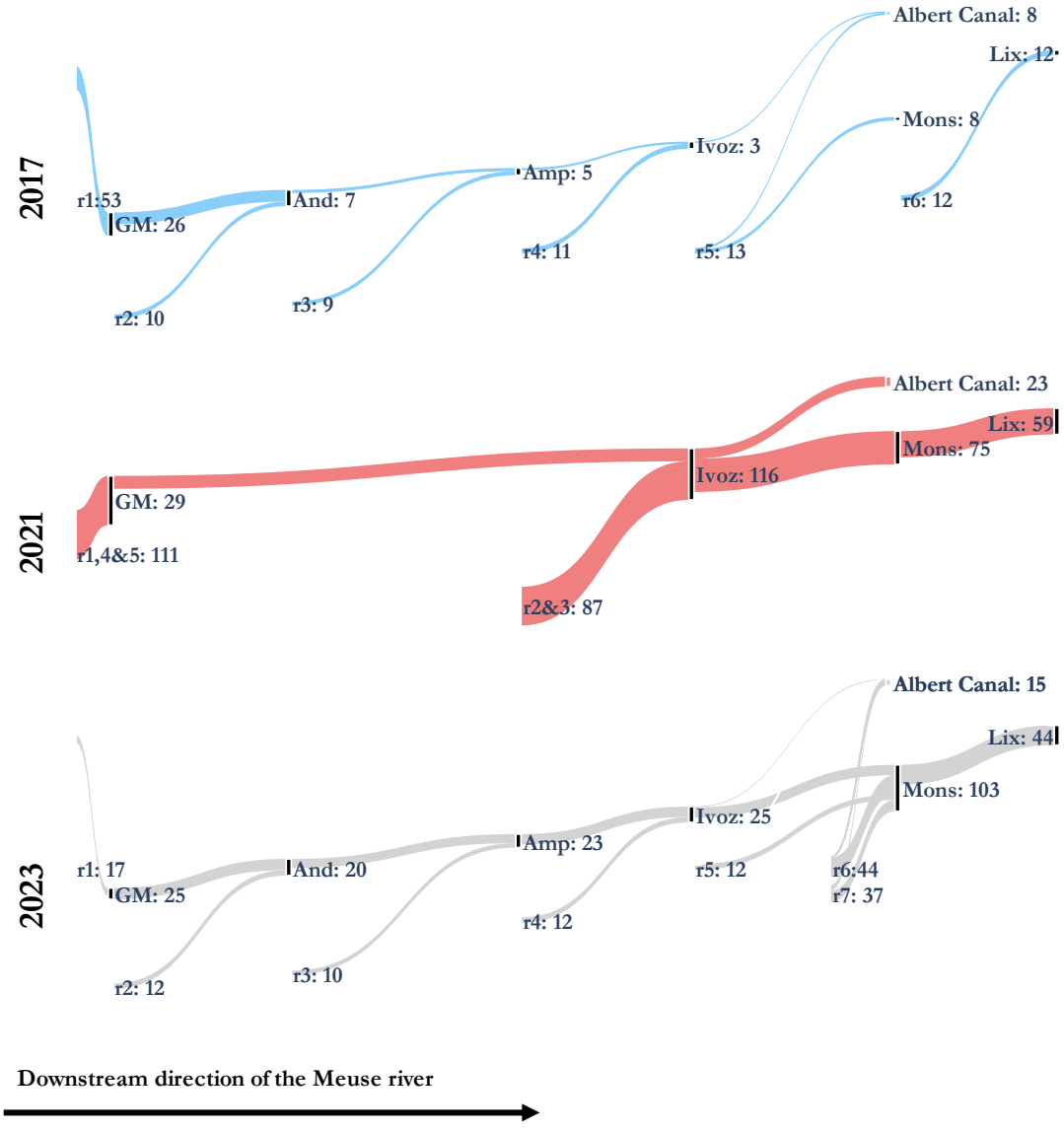

Figure 2: Recorded seaward journeys of smolts between successive dams of the mid-lower Meuse River for each experimental year**. With r:** release of smolts, **GM:** Grands-Malades dam**, And:** Andenne dam**, Amp:** Ampsin dam**, Mons:** Monsin dam**, and Lix:** Lixhe dam. The number behind the site's name differentiates smolt journeys from upstream releases and those released in the same reach. Forty-one smolts were not detected at the dam immediately downstream of their release point but in the subsequent reaches.

178 The hatchery-reared smolts were tracked using acoustic telemetry. This tracking was achieved through
179 transmitters implanted in each fish and a network of hydrophones. The hydrophones were positioned
180 at each dam, as well as at six other sites within reaches namely: the Tihange nuclear power plant (NPP),
181 the Albert canal, the Ourthe confluence, the Atlas bridge, the Boverie park. For each fish, the
182 transmitter was implanted via a small incision, approximately 1 cm in length, located between the
183 pelvic and pectoral fins (Roy et al., 2017; Lerquet et al., 2021). The transmitter weighed 0.6 g which
184 was less than 3% of the smallest smolt weight (Life4Fish, 2023; Renardy et al., 2023a). After the
185 implantation, the incision was closed with a resorbable suture (Renardy et al., 2023a). To ensure proper
186 scarring, a healing solution with antibiotic and antifungal properties was applied to the operated area
187 (Roy et al., 2017). The smolt was then placed in a recovery tank equipped with an oxygenator, and its
188 behaviour was monitored at regular intervals.

189 The hydrophones used were of two brands: LOTEK WHS 4250, except at Ivoz-Ramet and Monsin water
190 intakes, where ATS hydrophones (SR3017: onshore and SR3001: offshore) were used from 2021
191 onwards (Roy et al., 2017; Lerquet et al., 2021). The hydrophones were attached by a cable either to a
192 riverbank, or the abutment of a dam, or to a 500 kg wagon wheel placed on the riverbed. The
193 hydrophones were positioned 1 metre above the riverbed and the position was signalled at the surface
194 by a buoy (Lerquet et al., 2021).

195 Smolts were released at the beginning of reaches in small groups called releases. These releases helped
196 to sustain the population sample monitored in each reach. By adding new smolts, they filled the gap
197 left by upstream losses in the sample. In total, 19 releases were conducted: 6 in 2017, 5 in 2021, and 8
198 in 2023. The final release of 2023 between the Monsin and Lixhe dams was removed from the analyses
199 due to hydrophone failures in the reach. For every individual, a detection file in a text format recorded
200 the evolution of detections at various sites. On average, there were 3 448 detections per individual
201 (median value with min = 2, max = 145 841). The Sankey graphs in **Figure 2** illustrate the trajectories of
202 smolts migrating downstream at each site and their origin within the reach. Smolt lengths and masses

were also recorded during the tagging process. Both characteristics were analysed to understand the variability of physical conditions throughout the 3 experimental years.

2.3. Hydrodynamic data

To get knowledge about flow conditions faced by the smolts, hydraulic numerical modelling was performed. The one-dimensional (1D) model (Wolf1D) employed in this study solves the Saint-Venant equations using the finite volume method. It is part of the WOLF software (Archambeau et al., 2024), developed by the Hydraulics in Environmental and Civil Engineering (HECE) research group at the University of Liège. The WOLF software has been validated through numerous industrial projects and scientific publications (Erpicum et al., 2010; Goffin et al., 2020; Dewals et al., 2023; Renardy et al., 2023a). The primary inputs for the 1D model include river cross-sections, boundary conditions, flow infiltrations, initial conditions, and friction coefficients.

For this study, cross-sections were generated every 100 metres along the mid-lower Meuse River. The inclusion of infrastructures likely to disrupt the flow was also ensured. Each cross-section was built from bathymetric data with a resolution of 1x1 m, extracted from sonar surveys conducted by the Public Service of Wallonia (SPW). The model was subdivided into six sub-models due to the presence of dams, as depicted in **Figure 3 a & b**. Only the first sub-model began mid-reach, a few metres upstream of the Jambes bridge. The others extended over the reaches, with the upstream boundary at the downstream side of the upstream dam and the downstream boundary at the upstream side of the downstream dam as depicted in **Figure 3 a & b**.

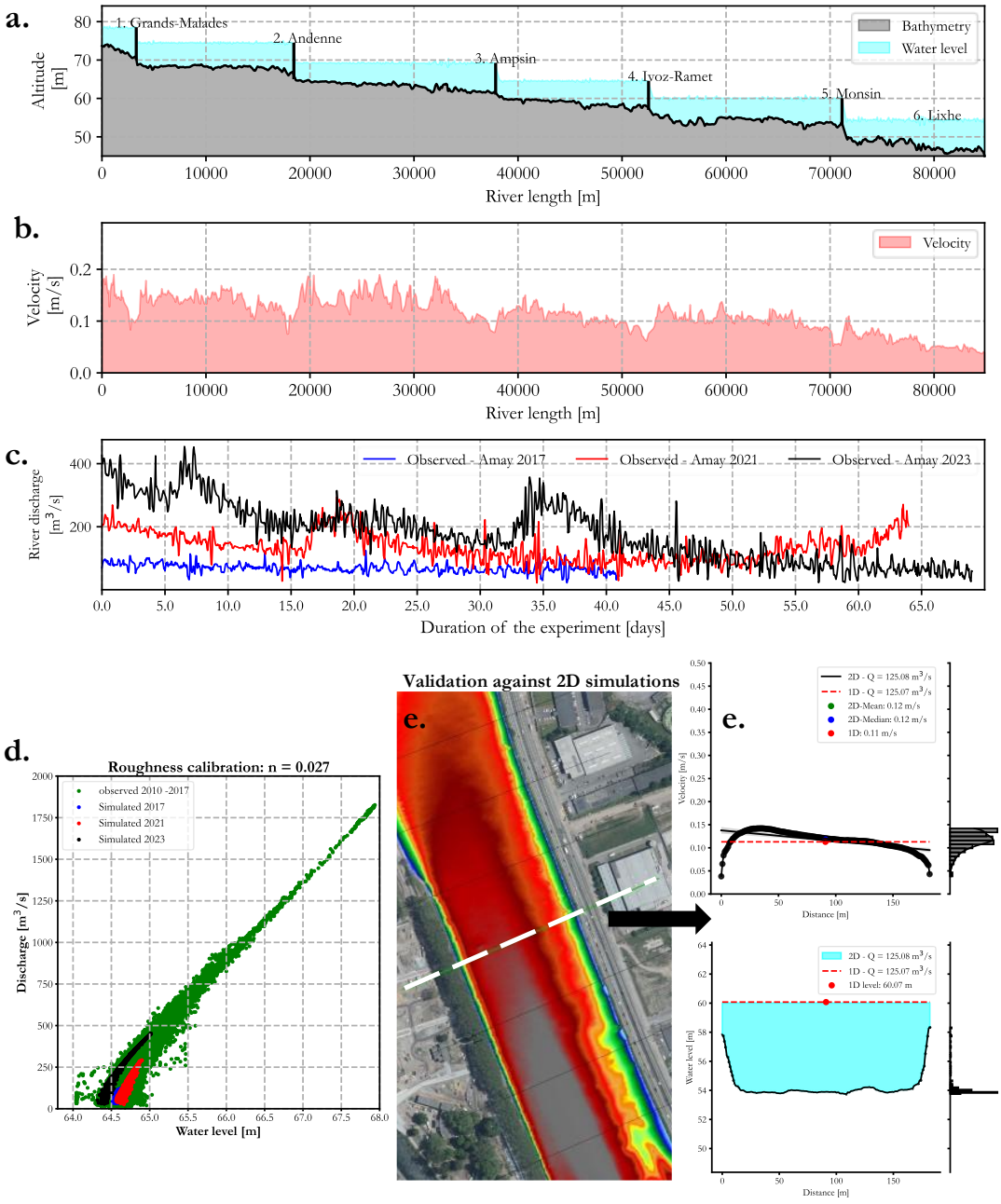

222

223 **Figure 3:** The 1D model. With, **a.** Simulated water levels along the 82 km of the mid-lower Meuse River
224 for a given time step, **b.** Simulated water velocities for the same time step, **c.** Observed hydrographs at
225 Amay hydrometric station during the three experiments, **d.** Calibration of the friction coefficients used
226 in the 1D model, **e.** Validation of the 1D simulated results against existing 2D simulations.

227 To ensure model continuity, the output hydrograph from the upstream sub-model was used as the
228 input for the downstream model. Also, throughout the three experimental years, the water levels at
229 dams varied temporally by no more than 1 cm. Thus, the average water levels observed near dams

were used as downstream boundary conditions of the sub-models. The only exception was the reach between Grands-Malades and Andenne dams, where the maximum elevation of the Andenne dam was used as the downstream boundary condition. The reason was the absence of a hydrometric station in the vicinity of the dam.

Regarding discharges, the flow contributions from major tributaries shown in **Figure 1** and the subtraction of water from the Albert Canal were extracted from the hourly hydrograph of their nearest hydrometric station (SPW, 2024). The only exception was the upper Meuse River for which the hydrographs were the differences between measurements at Amay station (**Figure 3 c**) and the upstream tributaries, respectively phase shifted. The lag time between distant observations was accounted for in reconstructing the upper Meuse River hydrographs. For each experiment, the computed difference was the discharge injected at the most upstream cell of the first 1D sub-model. After filtering out anomalies, the other hydrographs were injected into the corresponding cells of the sub-models. The initial conditions for each sub-model were obtained by pre-calculating a steady-state solution. The pre-calculated solution represented the first-time step of the simulation, as shown in **Figure 3 a & b**.

The calibration of the friction coefficients was based on hourly observations of flow rates and water levels measured at the Amay and Neuville stations from 2010 to 2017. The Manning coefficient obtained through this method was 0.027, as shown in **Figure 3 d**. This coefficient was extrapolated to all sub-models due to a lack of gauging stations. The results of the 1D model were validated by comparing the simulated velocities and water levels with those from existing two-dimensional (2D) simulations, as depicted in **Figure 3 e**. The comparison showed that the simulated water levels by both methods were similar, and the velocities had only 1% difference with the mean and median normal velocities calculated in 2D for the same section. The simulated results (water level, velocity, discharges, water depth, Froude number, and wetted section) were saved as one-dimensional matrices to facilitate their use.

2.4. Water temperature data

The water temperature in the Meuse River was monitored at four sites: Huy, Angleur, Monsin, and Lixhe as shown in **Figure 4**. The collected data encompassed the time periods of all three experiments of this study as shown in **Figure 4**. The exception was the Angleur station, where only the years 2021 and 2023 were available. Temperature observations were extrapolated to adjacent reaches expected to exhibit similar thermal variations due to the presence of two strong spatial gradients. These noticeable temperature gradients were attributed to the discharge of warm water from the Tihange nuclear power plant, followed by the influx of cold water from the Ourthe River a few kilometres downstream.

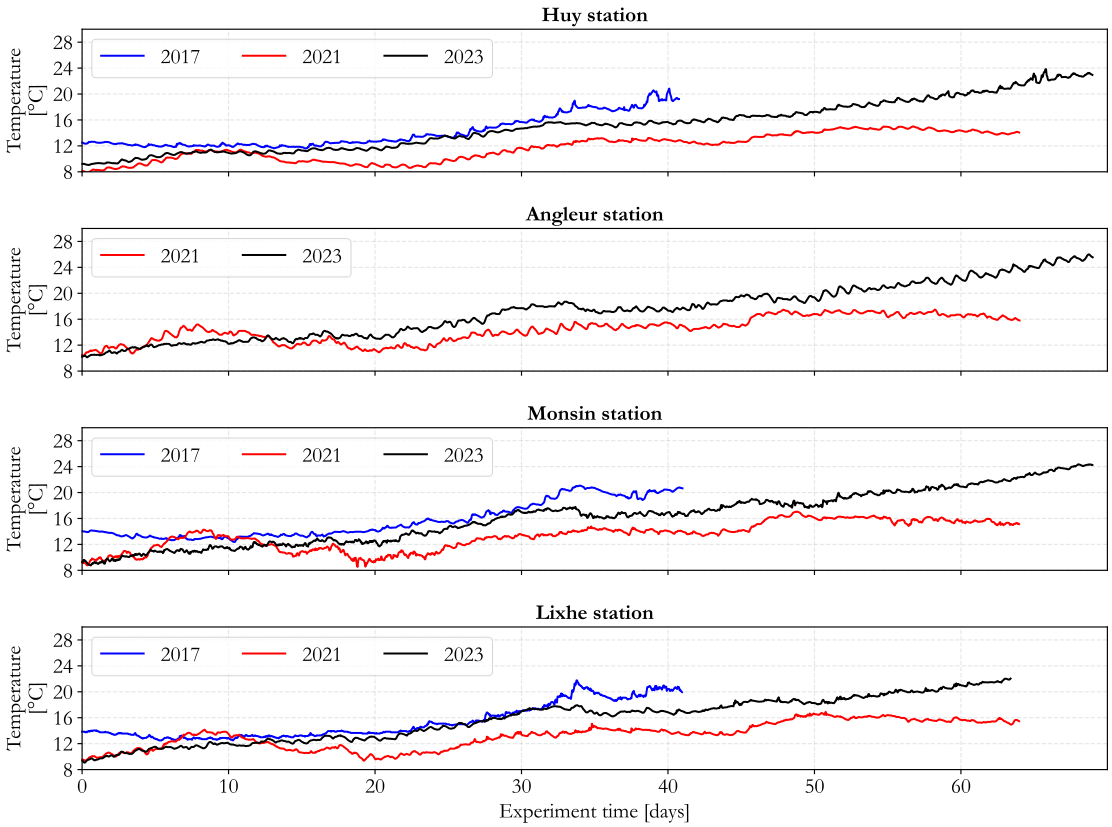

Figure 4: Recorded water temperatures during the 3 experiments from upstream to downstream.

2.5. Diel pattern data

The impact of light on smolts was evaluated using nychthemeral classification of detections. For each detection, the specific day was divided into daytime and nighttime based on the computed sunrise and sunset times at the detection sites (Kobyshev et al., 2017). The detection was then categorized as one of the two period according to the detection time. **Figure 5** illustrates the application of this method to the first detection of smolts at detection sites during the 3 experimental years.

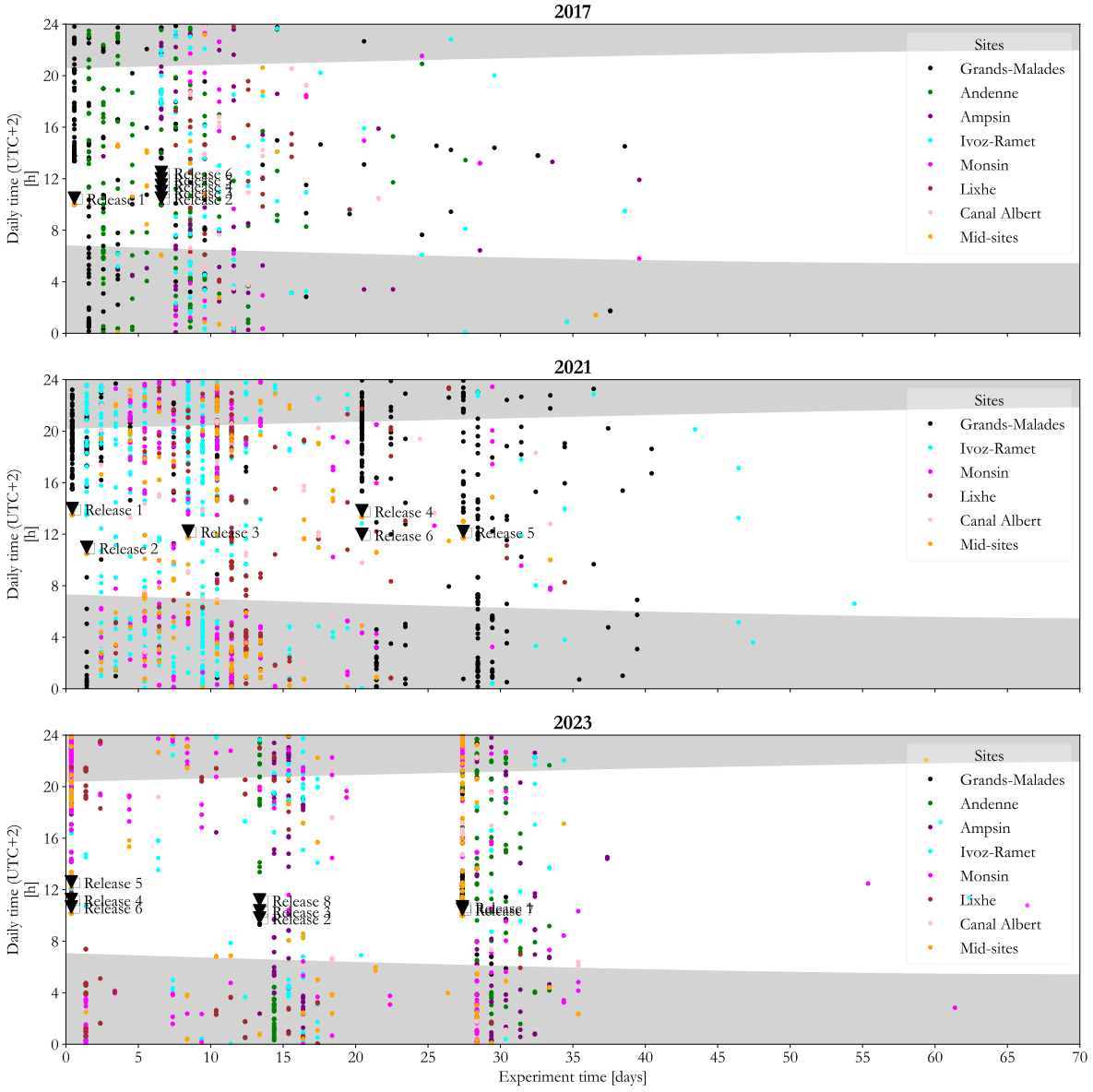

Figure 5: Diurnal pattern of first detections of smolts at different sites. The shaded areas represent nighttime during the three experiments.

2.6. Data treatment

2.6.1. Data preparation

The integration of ichthyological data with hydrodynamic data was accomplished through Python operations (Van Rossum & Drake Jr, 1995). First, smolts trajectories were reconstructed from detection data. Second, the mean flow velocities within reaches were directly associated with the respective

trajectories. The mean flow velocity between two detection sites was calculated as the velocity of a water particle moving from one site to the next concurrently with the smolt. Third, the water temperature within the reach and the nychthemeral classification of the detection were linked to each point of the trajectory. Finally, all smolts data were merged into a single database.

The variables derived from the database were:

a) **Body length:** The smolt length measured on a graduated scale.
b) **Mass:** The smolt mass measured on a scale.
c) **Migrated distance:** The linear distance travelled by the smolt along the river.
d) **Migration time:** The duration taken by the smolt to cover the migrated distance.
e) **Migration speed:** The ratio of the migrated distance to the migration time of the smolt.
f) **Distance between sites:** The distance travelled by the smolt between two detection sites within the same reach.
g) **Time between sites:** The duration taken by the smolt to travel the distance between sites.
h) **Traveling speed:** The ratio of the distance between sites to time between sites.
i) **Flow velocity:** The mean velocity encountered by the smolt during its journey between two sites.
j) **Relative speed:** The difference between the traveling speed and the flow velocity. This variable assessed whether the smolt was faster (positive value) or slower (negative value) than the flow.
k) **Water temperature:** The measured water temperature in the reach at the time of the detection.
l) **Nychthemeral classification:** The categorisation of the smolt detection as either diurnal or nocturnal.
m) **Research time:** The time spent upstream of an obstacle in the quest of a migration route.
n) **Overall migration speed:** The smolt migration speed along the linear path of the Mid-lower Meuse River. The overall migration speeds include the research time near obstacles.

2.6.2. Data analyses

The travelling speeds, relative speeds, and overall migration speeds of smolts were compared to flow velocities to determine the influence of flow velocity on smolt migration speed. The speeds of smolts and the flow velocities were normalized by the body length of the respective smolt to ensure comparability and transferability of the results, with both velocity units (body lengths per second [B.L./s] and meters per second [m/s]) being analysed. Negative traveling speeds, indicating upstream swimming, were categorized as disorientations. The flow velocity threshold of 0.15 m/s, recommended by the literature as the point below which smolt disorientations occur, was also tested (Renardy et al., 2021; Ben Jebria et al., 2023). Comparisons with traveling speeds provided insights into the links between flow velocities and seaward migration speeds in the absence of obstacles, while comparisons with overall migration speeds accounted for research time at barriers. Additionally, comparisons with relative velocities explained smolt travel modes (faster or slower than the flow). Water temperatures and the diurnal classification of first detections were included in the analyses to better explain smolt behaviours.

Graphical analyses, correlation matrices, principal component analyses (PCA), and multiple linear regression models were employed to analyse variable relationships. Scatter plots and probability density functions (PDFs) were plotted to visualize these relationships and data distributions. The Spearman non-parametric test was used for all correlation matrices due to the non-normal data distribution (Shapiro-Wilk normality test, $p < 0.001$, $n = 491$ smolts & $n = 986$ trajectories). Given the complexity of interpreting the Spearman test, the Pearson correlation test was also conducted to monitor the linear relationship between variables. Complex data transformations were avoided to preserve the straightforward interpretation of results. PCA and multiple linear regression models were performed on the entire database and each experimental year, after removing obviously correlated variables. The variables removed included mass, which was strongly correlated with length, and normalised velocities and speeds in body length per second, which were secondary computations. From PCA, correlation circles were plotted to explain relationships between variables. Linear modelling

confirmed relationships suggested by graphical analyses, correlation matrices, and PCA. Analyses were performed using Python (Van Rossum & Drake Jr, 1995) and R software (R Core Team, 2023).

3. Results

3.1. The sample

Among the 584 smolts released, 84.08% (n = 491 smolts) were detected by the tracking system and had valid migration trajectories. Within this sample, 40.73% (n = 200 smolts) were from the 2021 survey, 34.22% (n = 168 smolts) were from the 2023 survey, and 25.05% (n = 123 smolts) were from the 2017 survey. The trajectories of these smolts described 1,015 journeys between two successive detection sites. As shown in **Figure 2**, the lack of detection stations at the Andenne and Ampsin dams in 2021 led to the exclusion of 2.86% (n = 29) of the 1,015 trajectories between sites. Of the remaining 986 trajectories, 45.54% (n = 449 trajectories) were from the 2021 survey, 33.47% (n = 330 trajectories) were from the 2023 survey, and 20.99% (n = 207 trajectories) were from the 2017 survey.

The lengths and masses of the detected smolts varied across the experiments. Overall, the average length of the detected smolts was 155.71 mm (min = 135 mm, max = 188 mm) and the average mass was 38.63 g (min = 24 g, max = 65 g). The smolts exhibiting the greatest length were recorded during the 2021 survey, with an average length of 162.42 mm (std = 9.42 mm), compared to 151.78 mm (std = 6.05 mm) in 2023 and 150.19 mm (std = 3.71 mm) in 2017. The smolts with the greatest mass were also recorded during the 2021 survey, with an average mass of 42.55 g (min = 28 g, max = 65 g), compared to 34.13 g (min = 24 g, max = 54 g) in 2023 and 38.38 g (min = 33.7 g, max = 47.5 g) in 2017. The lengths and masses of smolts were strongly correlated (Spearman $\rho = 0.84$ | Pearson $r = 0.88$, $p < 0.01$, $n = 491$).

3.2. Smolts traveling speed between successive sites

The traveling speeds of smolts between two sites were positively correlated with flow velocities (Spearman $\rho = 0.27$ | Pearson $r = 0.24$, $p < 0.01$, $n = 986$), as shown in **Figure 6**. In 2017, the lowest flow

velocities were recorded, with a median of 0.11 m/s (0.76 BL/s), and the lowest traveling speeds, with a median of 0.11 m/s (0.69 BL/s). In 2021, the median flow velocity was 0.16 m/s (1.03 BL/s), and the median traveling speed was 0.16 m/s (1.01 BL/s). The highest values were in 2023, with a median flow velocity at 0.3 m/s (1.98 BL/s) and median traveling speed at 0.19 m/s (1.29 BL/s). Overall, the median traveling speed was 0.15 m/s (0.95 BL/s), and the median flow velocity was 0.13 m/s (0.90 BL/s). Nevertheless, principal component analyses and correlation matrices revealed a decreasing correlation between the two variables across the three experiments. The traveling speeds of smolts were more correlated with flow velocities in 2017 (Spearman $\rho = 0.49$ | Pearson $r = 0.43$, $p < 0.01$, $n = 207$) than in 2021 (Spearman $\rho = 0.13$ | Pearson $r = 0.22$, $p < 0.01$, $n = 449$) and 2023 (Spearman $\rho = 0.05$ | Pearson $r = 0.04$, $p \leq 0.5$, $n = 330$), as depicted by the correlation circles in **Figure 6**. For all correlation circles, the first two principal components explained more than 56% of the data variability.

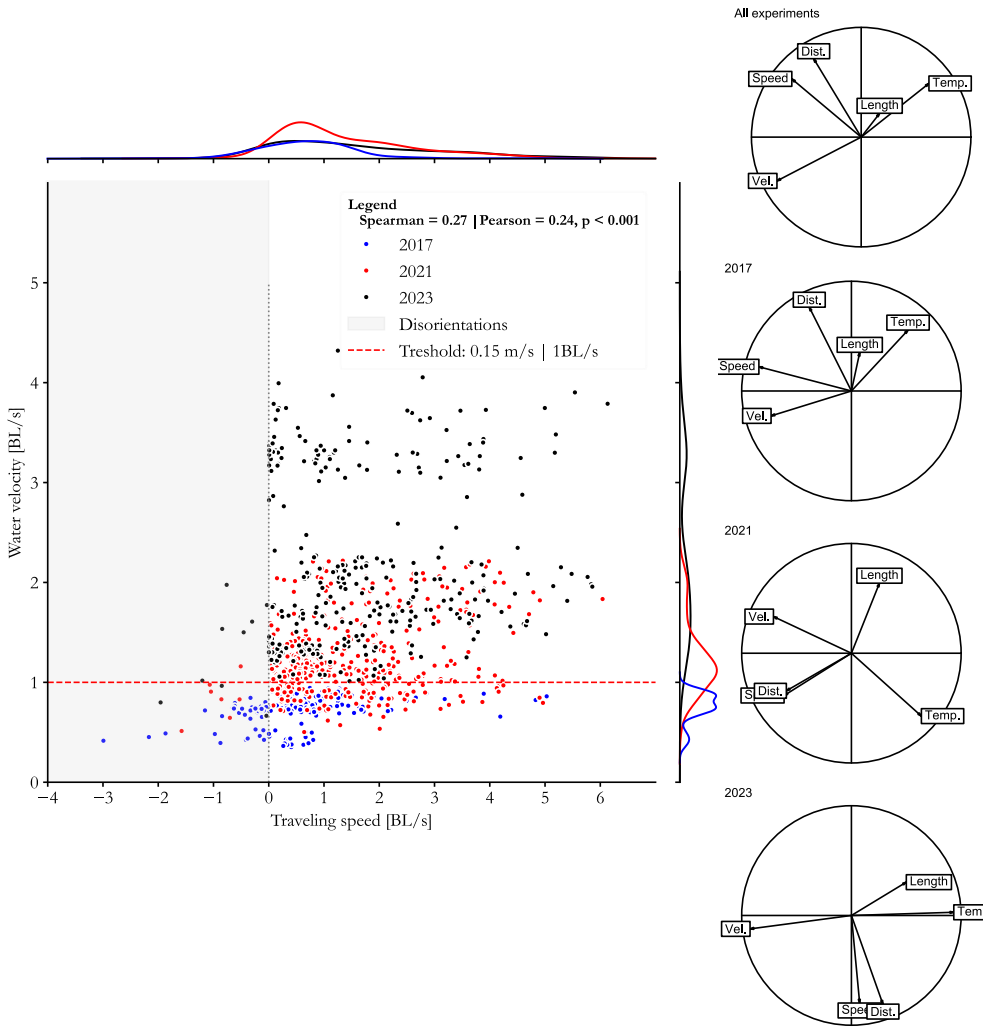

Figure 6: Influence of water velocity on smolts traveling speed. Correlation circles explain the relationships between variables with Vel.: water velocity, Length: smolt length, Temp.: water temperature, Dist: distance already migrated by the smolt.

Among the 986 journeys of smolts between successive detection sites, 6.29% (n = 62) were disorientations, defined as upstream movements of smolts. Of these disorientations, 88.71% (n = 55) occurred at flow velocities below the threshold of 0.15 m/s| 1 BL/s, as depicted in **Figure 6**. Despite its lower representation in the sample, 74.19% (n = 46) of these disorientations were from the 2017 experiment, compared to 11.29% (n = 7) in 2021 and 14.52% (n = 9) in 2023.

Among the variables influencing smolt traveling speed between detection sites, the distance already migrated was the most correlated. Traveling speeds were positively correlated with distances migrated

(Spearman ρ = 0.47 | Pearson r = 0.35, p < 0.01, n=986). Regarding the diel pattern, 53.65% of smolts reached detection sites at night. In 2017, 35.75% of smolts were first detected at night, compared to 57.02% in 2021 and 60.30% in 2023. Smolts that reached the next detection sites during daytime were generally faster (median = 1.23 BL/s, min = -2.17 BL/s, max = 5.86 BL/s) than those that reached detection sites during nighttime (median = 0.76 BL/s, min = -2.99 BL/s, max= 6.13 BL/s).Thus, daytime periods of first detection were positively correlated with traveling speeds (Spearman ρ = 0.11 | Pearson r = 0.05, p < 0.01, n=986). Conversely, traveling speeds were negatively correlated with water temperatures (Spearman ρ = -0.1 | Pearson r = -0.07, p ≤ 0.03, n = 986). Besides, linear regression models highlighted the influence of water velocity and migrated distance on traveling speed as shown in **Table 2**. The effect of water velocity was considerable in the 2017 model, noticeable in the 2021, and inexistant in the 2023 model. Similarly to PCA, the 2017 and 2023 models suggested a negative influence of increasing water temperatures on the traveling speed of smolts as shown in **Table 2**.

Table 2: Multiple linear regression models fitted to explain smolts traveling speed from other variables. With, $\boldsymbol{Vel.}$: water velocity (m/s), $\boldsymbol{Dist.}$: Distance already migrated by the fish (m), $\boldsymbol{Temp.}$: Temperature (°C), $\boldsymbol{Len.}$: smolt length (mm)

Dataset	Best multiple linear regression model for traveling speed by A.I.C..	R^2	Adj. R^2
Whole	$5.638 \times 10^{-2} + 3.815 \times 10^{-1}\boldsymbol{Vel.} + 3.593 \times 10^{-6}\boldsymbol{Dist.}$	0.1701	0.1684
2017	$6.300 \times 10^{-2} + 2.569\,\boldsymbol{Vel.} - 2.212 \times 10^{-2}\,\boldsymbol{Temp.} + 3.831 \times 10^{-6}\boldsymbol{Dist.}$	0.3152	0.3051
2021	$2.809 \times 10^{-1} + 6.129 \times 10^{-1}\boldsymbol{Vel.} - 1.451 \times 10^{-3}\,\boldsymbol{Len.} + 2.293 \times 10^{-6}\boldsymbol{Dist.}$	0.1288	0.123
2023	$-2.255 \times 10^{-1} - 1.068 \times 10^{-2}\,\boldsymbol{Temp.} + 3.398 \times 10^{-3}\,\boldsymbol{Len.} + 5.633 \times 10^{-6}\boldsymbol{Dist.}$	0.1691	0.1615

3.3. Smolts relative speeds

The relative speeds of smolts compared to the flow were negatively correlated with flow velocities (Spearman ρ = -0.21 | Pearson r = -0.34, p < 0.01, n = 986), as illustrated in **Figure 7**. In all three experiments, smolts were generally slower than the flow. The highest relative speeds were recorded in 2017, with a median of -0.01 m/s (-0.04 BL/s). In 2021, the median was -0.04 m/s (-0.23 BL/s), while in

2023, it was -0.10 m/s (-0.68 BL/s). The overall median relative speed of smolts was -0.05 m/s (-0.30 BL/s). In addition, a negative correlation (Spearman $\rho = -0.42$ | Pearson $r = -0.53$, $p < 0.01$, $n = 188$) was observed at detection sites located in the middle of reaches, far from dams. The multiple linear regression models and the PCA also revealed a weak negative correlation between the relative speed of smolts and the water velocity, as shown in **Figure 7** and **Table 3**. According to the models, the strongest influence of flow velocity was in 2023, and the weakest was in 2017. For the PCA, the first two principal components used to plot the corelation circles explained more than 54% of the data variability for each dataset. For other variables, the relative speeds were positively correlated with travelling speeds (Spearman $\rho = 0.84$ | Pearson $r = 0.85$, $p < 0.01$, $n = 986$) , distances already migrated by the smolts (Spearman $\rho = 0.37$ | Pearson $r = 0.32$, $p < 0.01$, $n = 986$) , and water temperatures (Spearman $\rho = 0.11$ | Pearson $r = 0.16$, $p < 0.01$, $n = 986$) .

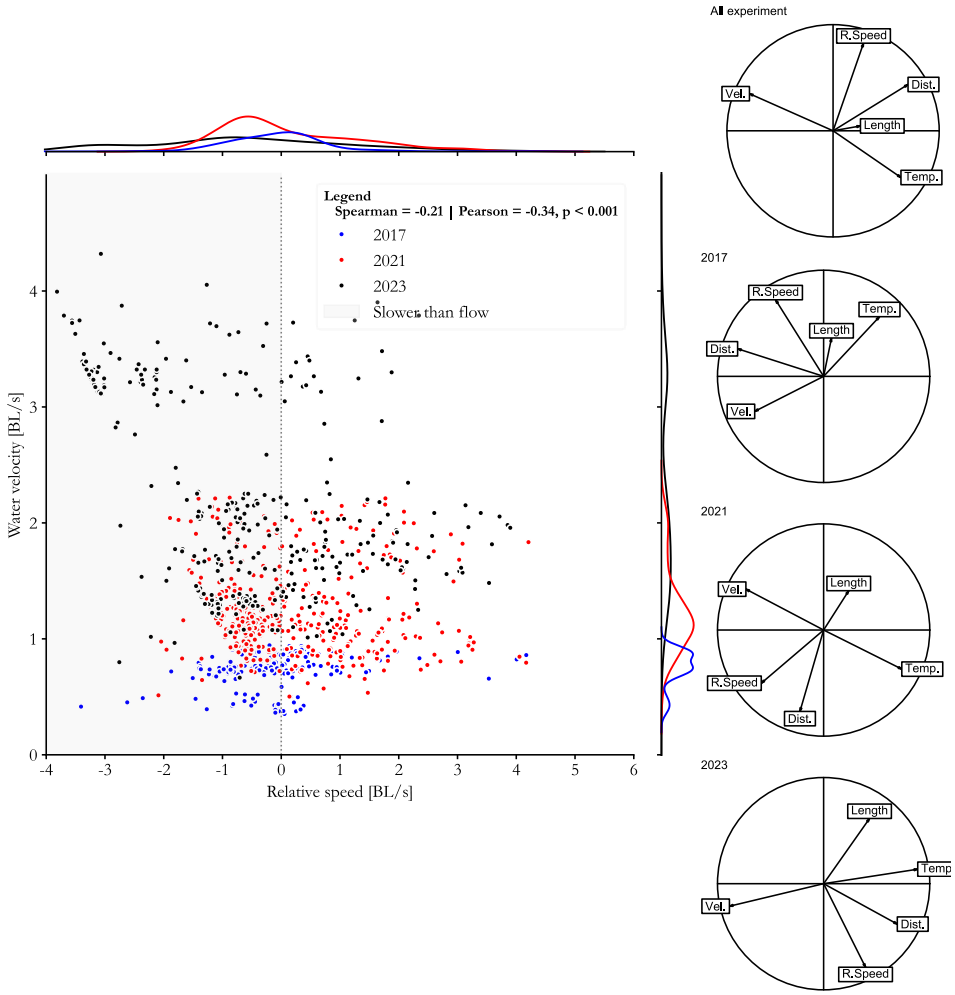

411

412 **Figure 7:** Influence of water velocity on the relative speed of smolts compared to the flow. Corelation
413 circles explain the relationships between variables with (R. speed: smolt relative speed, Vel.: water
414 velocity, Length: smolt length, Temp.: water temperature, Dist.: distance already migrated by the
415 smolt).

416 **Table 3:** Multiple linear regression models fitted to explain the relative speed of smolts from other
417 variables. With, $\boldsymbol{Vel.}$: water velocity (m/s), $\boldsymbol{Dist.}$: Distance already migrated by the fish (m), $\boldsymbol{Temp.}$:
418 Temperature (°C), $\boldsymbol{Len.}$: smolt length (mm).

Dataset	Best multiple linear regression model for relative speed by A.I.C.	R^2	Adj. R^2
Whole	$5.638 \times 10^{-2} - 6.185 \times 10^{-1}\boldsymbol{Vel.} + 3.593 \times 10^{-6}\boldsymbol{Dist.}$	0.2178	0.2163
2017	$6.300 \times 10^{-2} + 1.569\,\boldsymbol{Vel.} - 2.212 \times 10^{-2}\,\boldsymbol{Temp.} + 3.831 \times 10^{-6}\boldsymbol{Dist.}$	0.2313	0.3051
2021	$2.809 \times 10^{-1} - 3.874 \times 10^{-1}\boldsymbol{Vel.} - 1.451 \times 10^{-3}\,\boldsymbol{Len.} + 2.293 \times 10^{-6}\boldsymbol{Dist.}$	0.08911	0.08297

2023	$-4.321 \times 10^{-1} - 7.741 \times 10^{-1}\boldsymbol{Vel.} - \mathbf{3.373 \times 10^{-3}}\boldsymbol{Len.} + 5.450 \times 10^{-6}\boldsymbol{Dist.}$	0.3265	0.3203

419

420 ### 3.4. Overall migration speeds

421 The overall migration speed of smolts, accounting for research time at barriers, was positively
422 correlated with flow velocity (Spearman ρ = 0.46 | Pearson r = 0.49, p < 0.01, n = 485) , as shown in
423 **Figure 8**. During the three experimental years, migration speeds were low in 2017 (0.02 m/s | 0.15
424 BL/s), moderate in 2021 (0.05 m/s | 0.33 BL/s), and high in 2023 (0.12 m/s | 0.74 BL/s). The overall
425 median migration speed was 0.05 m/s (0.34 BL/s). The correlation between migration speed and water
426 velocity was the lowest in 2017 (Spearman ρ = 0.05| Pearson r = 0.08, p ≤ 0.39, n = 123), intermediate
427 in 2021 (Spearman ρ = 0.22 | Pearson r = 0.16, p ≤ 0.03, n = 200) , and the highest in 2023 (Spearman
428 ρ = 0.23 |Pearson r = 0.28 (p < 0.01, n = 162). These variations are illustrated by correlation circles in
429 **Figure 8**. Migration speed was positively correlated with the distance already migrated (Spearman ρ =
430 0.38 | Pearson ρ = 0.14, p < 0.01, n = 485). Conversely, it was negatively correlated with research time
431 at barriers (Spearman ρ = -0.59| Pearson r =-0.30, p < 0.01, n = 485) and water temperature (Spearman
432 ρ = -0.19 | Pearson r = -0.25, p < 0.01, n = 485) , as depicted in **Figure 8**. Research time at barriers was
433 also negatively correlated with flow velocity encountered by smolts (Spearman ρ = -0.39 | Pearson r =
434 -0.08, p < 0.01, n = 485). Additionally, the multiple regression model fitted on the entire dataset
435 highlighted the influence of water velocity, research time, and distance already migrated by smolts on
436 migration speeds as shown in **Table 4**. All fitted models indicated the negative influence of research
437 time at barriers, with the strongest influence in 2017 model and the weakest in 2023 model as shown
438 in **Table 4**.

439

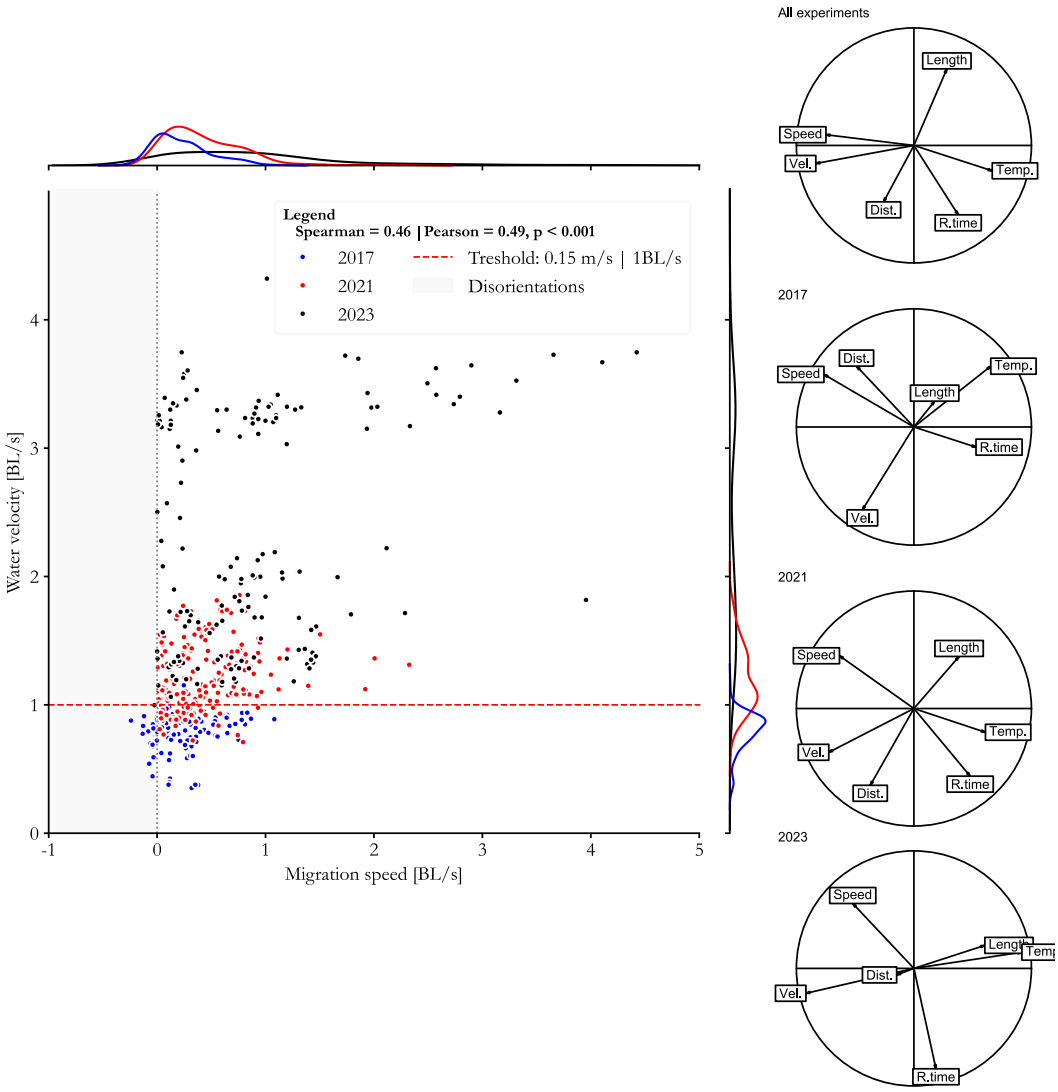

Figure 8: Influence of water velocity on the migration speed of smolts. Corelation circle explain the relationships between variables with (R. speed: smolt relative speed, Vel.: average water velocity, Length: smolt length, Temp.: average water temperature, Dist.: distance already migrated by the smolt, R.time : average research time near obstacles).

Table 4: Multiple linear regression models fitted to explain the migration speed of smolts from other variables. With, ***Vel.***: water velocity (m/s), ***Dist.***: Distance already migrated by the fish (m), ***Temp.***: Temperature (°C), ***Len.***: smolt length (mm), ***Res.***: research time at barriers.

Dataset	Best multiple linear regression model for migration speed by A.I.C.	R^2	Adj. R^2

Whole	$9.456 \times 10^{-3} + 3.441 \times 10^{-1}\boldsymbol{Vel.} \ -1.542 \times 10^{-4}\boldsymbol{Res.} + 3.469 \times 10^{-6}\boldsymbol{Dist.}$	0.2947	0.2903
2017	$2.156 \times 10^{-1} - 1.247 \times 10^{-3}\boldsymbol{Len.} - 8.967 \times 10^{-5}\ \boldsymbol{Res.} \mp 1.390 \times 10^{-6}\boldsymbol{Dist.}$	0.3699	0.354
2021	$1.994 \times 10^{-1} - 9.731 \times 10^{-3}\ \boldsymbol{Temp.} - 2.130 \times 10^{-4}\boldsymbol{Res.}$	0.2067	0.1986
2023	$3.146 \times 10^{-1} - 1.467 \times 10^{-2}\boldsymbol{Temp.} \ -1.470 \times 10^{-4}\boldsymbol{Res.} + 7.485 \times 10^{-7}\boldsymbol{Dist.}$	0.1664	0.1505

4. Discussion

By integrating smolt trajectories from acoustic telemetry with numerically reconstructed hydrodynamic conditions, this study examined the impact of various flow velocities on smolt migration. Also, it evaluated how water temperature, the diel pattern, and migrated distance influence migration speeds. The study underscores the relative positive effect of flow velocity on smolt downstream migration, as documented in the literature (Thorstad et al., 2012; Silva et al., 2020; Renardy et al., 2021; Ben Jebria et al., 2023). The results confirmed the general positive correlations between migration speeds and flow velocities as well as upstream movements at low flow velocities. They also showed that smolts are generally slower than the flow particularly at high flow velocities. The investigation suggested that migration speed is positively correlated with migrated distance but negatively with water temperature. Additionally, first detections of smolts at detection sites were generally nocturnal reflecting the nocturnal migratory behaviour of hatchery smolts.

The traveling speeds of smolts between two successive detection sites without obstacles generally increase with flow velocities. It was shown by the positive correlation between the two variables. Nevertheless, the correlation was stronger at low flow velocity conditions as demonstrated by the 2017 survey but decreased in 2021 and almost disappeared at relatively high flow velocities in 2023. These observations suggest an optimal water velocity range for smolt in rivers above which high velocities impede the migration speed. For instance, in 2023, several smolts exhibited exceptionally low downstream migration speeds at flow velocities above 3 BL/s. These results are consistent with Renardy et al. (2023b), who observed also very slow downstream migration speeds of smolts at very high flow velocities in a bypass channel. In summary, the results suggest that the flow velocity increases

the downstream migration speeds of smolts, provided it remains below a certain threshold (approximately 3 BL/s in this study).

Similarly, flow velocities below 1 BL/s disorient smolts. The three experimental years reveal that upstream movements occur at flow velocities below 0.15 m/s (1 BL/s). These results corroborate with Renardy et al. (2021) and Ben Jebria et al. (2023), who observed smolt disorientations at flow velocities below 0.15 m/s and 0.20 m/s, respectively. It worths noting that depending on smolt sizes in a specific river, 1 BL/s corresponds to flow velocities ranging between 0.13 and 0.20 m/s. In addition, the 2017 survey which was characterised by low flow velocities (< 0.20 m/s), accounted for 74% of upstream movements. This is in agreement with the observations of Honkanen et al. (2021) and Lilly et al. (2022) on numerous trajectories in the opposite direction of the seaward migration in standing waters. Thus, a flow velocity of one body length per second seems the minimum required to orient smolts downstream.

The traveling speed of a smolt between two successive detection sites is correlated with other explanatory variables. It increases with the distance already migrated by the smolt. The significant correlation (Spearman $\rho = 0.47$ | Pearson $r = 0.35$, p-value: < 0.01, n=986) between the distance already migrated and the traveling speed between two sites indicates an acceleration of the smolt throughout its downstream migration, probably due to the habituation and the smoltification process. Moreover, smolts were generally faster during the day (median = 1.23 BL/s) than at night (median = 0.76 BL/s), even though, most smolts travelled at night. This strategy could be explained by better visual cues for downstream migration during daylight compared to nighttime but also by the foraging tactic of juvenile salmon (Fraser et al., 1993). Regarding water temperature, the results suggest it was negatively but weakly correlated with the traveling speeds in the three experiments. Additionally, the four trajectories recorded when water temperatures exceeded 19°C were characterised by very low traveling speeds between two sites (maximum 0.15 BL/s). This aligns with Martin et al. (2012), who noted that hatchery smolts decelerate by 80% when water temperatures exceed 17°C. In summary, the results suggest that

the traveling speeds of smolts increases with the distance migrated and the daytime but decreases with water temperatures especially above 19°C.

The relative speeds of smolts compared to the flow decrease as the flow velocity increases. The results indicate that smolts migrate downstream generally slower than the flow. However, as flow velocities increase, the difference between the flow velocity and the smolts' traveling speeds also increases (Spearman $\rho = -0.21$ | Pearson $r = -0.34$, $p < 0.001$, $n = 986$). These findings suggest that smolts resist high flow velocities. Although counterproductive for rapid downstream migrations, this behaviour aligns with Ashraf et al. (2024), who postulated that increased flow velocity generally accelerates fish fatigue. Consequently, smolts spend energy resisting high flow velocities. The reasons for this tactic could also be related to smolts willing to control their downstream trajectories while avoiding dangers within the flow. Nevertheless, this behaviour joins the observations of Enders et al. (2009) and Erpicum et al. (2022) regarding positive rheotaxis near obstacles due to abrupt increases in flow velocities.

The overall migration speed of smolts in the mid-lower Meuse River increases with flow velocities. This correlation is due to the relationship between flow velocity and river discharges. In the mid-lower Meuse River, changes in discharge affect mostly water velocities but only slightly water levels. Consequently, smolts spent less time near obstacles when river discharges were high. In all experiments, it was shown by research times which were negatively correlated with the mean flow velocities. Research time at barriers also negatively influenced migration speed in all multiple regression models. As for traveling speeds, the overall migration speeds were correlated positively to the distances migrated by smolts.

5. Conclusion

Knowledge gap regarding the impact of river hydrodynamics on aquatic fauna movements contribute to fish species extinction and impede their sustainable reintroduction into human-altered rivers. This study sought to address part of that scientific gap. It characterised the impact of major environmental

conditions suggested by literature, on the downstream migration speed of 491 hatchery smolts crossing successively six dams along 82 km of the middle and lower Meuse River in Belgium. Over three hydrologically distinct years, the study combined smolt trajectories obtained via acoustic telemetry with numerically computed hydrodynamic conditions encountered by the smolts. It also considered the influences of water temperatures in the reaches and the nychthemeral cycle throughout the downstream migration of smolts.

The results show that the migration speed of smolts along a human-altered river is generally positively correlated with flow velocity. The water velocity within a reach guides juvenile Atlantic salmon downstream as long as it remains greater than the smolt's body length per second. Additionally, in this case study, relatively high flow velocities are caused by high discharges that facilitate the rapid crossing of obstacles by the smolts. However, relatively high flow velocities (above three body lengths per second) slowdown the smolts in comparison to the flow. The study also observes that the migration speed of smolts improves with the distance already migrated and that smolts migrate faster during the day than at night. Nevertheless, they generally migrate at night. As for increasing water temperatures, they negatively but very slightly impact migration speeds if they remain below 19°C and above the lowest temperature observed in the study, which is 8.75°C.

The main limitation of this study is the one-dimensional spatial discretisation of both smolt trajectories and numerical model. Indeed, the smolt positions follow only the river axis and were sometimes separated by several kilometres. This prevents knowledge of smolt activities within the reach and makes the use of more detailed hydrodynamic models, such as 2D and 3D, useless. Nevertheless, these results pave the way for establishing strong science-based policies regarding river environmental flows. By characterising the influences of flow velocity, temperature, and the nychthemeral cycle on smolt downstream migration, this study highlights the importance of establishing optimal detailed flow conditions in human-altered rivers for each of these variables during the migration window of smolts.

6. Acknowledgements

Funding: Utashi D. Ciraane acknowledges the FNRS for funding his PhD project as an FRS-FNRS PhD fellow (1.A.091.24F). The authors acknowledge the LIFE4FISH project for the smolts data. Damien Sonny, Marc Lerquet, Pierre Archambeau, Benjamin Dewals, Michel Pirotton, and Sébastien Erpicum participated in the LIFE4FISH project. The LIFE4FISH project was funded by the European Union LIFE program LIFE4FISH (LIFE16/NAT/ BE/000807).

7. References

Aldvén, D., Hedger, R., Økland, F., Rivinoja, P., & Höjesjö, J. (2015). Migration speed, routes, and mortality rates of anadromous brown trout Salmo trutta during outward migration through a complex coastal habitat. *Marine Ecology Progress Series*, *541*, 151–163. https://doi.org/10.3354/meps11535

Archambeau, P., Erpicum, S., Dewals, B., & Pirotton, M. (2024). *WOLF software*. https://wolf.hece.uliege.be/

Ashraf, M. U., Nyqvist, D., Comoglio, C., Nikora, V., Marion, A., Domenici, P., & Manes, C. (2024). Decoding burst swimming performance: A scaling perspective on time-to-fatigue. *Journal of The Royal Society Interface*, *21*(219), 20240276. https://doi.org/10.1098/rsif.2024.0276

Ben Ammar, I., Baeklandt, S., Cornet, V., Antipine, S., Sonny, D., Mandiki, S. N. M., & Kestemont, P. (2020). Passage through a hydropower plant affects the physiological and health status of Atlantic salmon smolts. *Comparative Biochemistry and Physiology Part A: Molecular & Integrative Physiology*, *247*, 110745. https://doi.org/10.1016/j.cbpa.2020.110745

Ben Jebria, N., Carmigniani, R., Drouineau, H., De Oliveira, E., Tétard, S., & Capra, H. (2023). Coupling 3D hydraulic simulation and fish telemetry data to characterize the behaviour of migrating smolts approaching a bypass. *Journal of Ecohydraulics*, *8*(2), 144–157. https://doi.org/10.1080/24705357.2021.1978345

Benitez, J.-P., Dierckx, A., Caparros Megido, R., Renardy, S., Vom Berge, C., P, H., Géraldine, J., Gelder, J., Nzau Matondo, B., Philippart, J.-C., & Ovidio, M. (2024). *Subvention d'etude relative a la rehabilitation du Saumon atlantique dans le bassin de la meuse. Rapport final février 2023—Janvier 2024*. https://orbi.uliege.be/handle/2268/318403

Benitez, J.-P., Dierckx, A., Rimbaud, G., Nzau Matondo, B., Renardy, S., Rollin, X., Gillet, A., Dumonceau, F., Poncin, P., Philippart, J.-C., & Ovidio, M. (2022). Assessment of Fish Abundance, Biodiversity and Movement Periodicity Changes in a Large River over a 20-Year Period. *Environments*, *9*(2), Article 2. https://doi.org/10.3390/environments9020022

Bjerck, H. B., Urke, H. A., Haugen, T. O., Alfredsen, J. A., Ulvund, J. B., & Kristensen, T. (2021). Synchrony and multimodality in the timing of Atlantic salmon smolt migration in two Norwegian fjords. *Scientific Reports*, *11*(1), 6504. https://doi.org/10.1038/s41598-021-85941-9

Bunt, C. M., Castro-Santos, T., & Haro, A. (2012). Performance of Fish Passage Structures at Upstream Barriers to Migration. *River Research and Applications*, *28*(4), 457–478. https://doi.org/10.1002/rra.1565

Chen, J., Shi, H., Sivakumar, B., & Peart, M. R. (2016). Population, water, food, energy and dams. *Renewable and Sustainable Energy Reviews*, *56*, 18–28. https://doi.org/10.1016/j.rser.2015.11.043

Chen, Q., Li, Q., Lin, Y., Zhang, J., Xia, J., Ni, J., Cooke, S. J., Best, J., He, S., Feng, T., Chen, Y., Tonina, D., Benjankar, R., Birk, S., Fleischmann, A. S., Yan, H., & Tang, L. (2023). River Damming Impacts on Fish Habitat and Associated Conservation Measures. *Reviews of Geophysics*, *61*(4), e2023RG000819. https://doi.org/10.1029/2023RG000819

Davidsen, J., Svenning, M.-A., Orell, P., Yoccoz, N., Dempson, J. B., Niemelä, E., Klemetsen, A., Lamberg, A., & Erkinaro, J. (2005). Spatial and temporal migration of wild Atlantic salmon smolts determined from a video camera array in the sub-Arctic River Tana. *Fisheries Research*, *74*(1), 210–222. https://doi.org/10.1016/j.fishres.2005.02.005

591 Dewals, B., Kitsikoudis, V., Angel Mejía-Morales, M., Archambeau, P., Mignot, E., Proust, S., Erpicum,
592 S., Pirotton, M., & Paquier, A. (2023). Can the 2D shallow water equations model flow intrusion into
593 buildings during urban floods? *Journal of Hydrology*, *619*, 129231.
594 https://doi.org/10.1016/j.jhydrol.2023.129231

595 Dolotov, S. I. (2006). The effects of water temperature on the migration of smolts of the Atlantic
596 salmon Salmo salar L. *Journal of Ichthyology*, *46*(2), S194–S203.
597 https://doi.org/10.1134/S0032945206110099

598 Doogan, A., Cotter, D., Bond, N., Ó'Maoiléidigh, N., & Brophy, D. (2023). Partitioning survival during
599 early marine migration of wild and hatchery-reared Atlantic salmon (Salmo salar L.) smolts using
600 acoustic telemetry. *Animal Biotelemetry*, *11*(1), 39. https://doi.org/10.1186/s40317-023-00352-z

601 Enders, E. C., Gessel, M. H., & Williams, J. G. (2009). Development of successful fish passage
602 structures for downstream migrants requires knowledge of their behavioural response to accelerating
603 flow. *Canadian Journal of Fisheries and Aquatic Sciences*, *66*(12), 2109–2117.
604 https://doi.org/10.1139/F09-141

605 Erpicum, S., Dewals, B., Archambeau, P., Detrembleur, S., & Pirotton, M. (2010). Detailed Inundation
606 Modelling Using High Resolution DEMs. *Engineering Applications of Computational Fluid Mechanics*,
607 *4*(2), 196–208. https://doi.org/10.1080/19942060.2010.11015310

608 Erpicum, S., Kitsikoudis, V., Archambeau, P., Dewals, B., & Pirotton, M. (2022). Experimental
609 Assessment of the Influence of Fish Passage Geometry Parameters on Downstream Migrating Atlantic
610 Salmon (Salmo salar) Smolts Behavior. *Water*, *14*(4), Article 4. https://doi.org/10.3390/w14040616

611 Fjeldstad, H. P., Uglem, I., Diserud, O. H., Fiske, P., Forseth, T., Kvingedal, E., Hvidsten, N. A., ØKland, F.,
612 & Järnegren, J. (2012). A concept for improving Atlantic salmon Salmo salar smolt migration past
613 hydro power intakes. *Journal of Fish Biology*, *81*(2), 642–663. https://doi.org/10.1111/j.1095-
614 8649.2012.03363.x

615 Franklin, P. A., Bašić, T., Davison, P. I., Dunkley, K., Ellis, J., Gangal, M., González-Ferreras, A. M.,
616 Gutmann Roberts, C., Hunt, G., Joyce, D., Klöcker, C. A., Mawer, R., Rittweg, T., Stoilova, V., &
617 Gutowsky, L. F. G. (2024). Aquatic connectivity: Challenges and solutions in a changing climate.
618 *Journal of Fish Biology*, *105*(2), 392–411. https://doi.org/10.1111/jfb.15727

619 Fraser, N. H. C., Metcalfe, N. B., & Thorpe, J. E. (1993). Temperature-dependent switch between
620 diurnal and nocturnal foraging in salmon. *Proceedings of the Royal Society of London. Series B:*
621 *Biological Sciences*, *252*(1334), 135–139. https://doi.org/10.1098/rspb.1993.0057

622 Gibeau, P., Connors, B. M., & Palen, W. J. (2017). Run-of-River hydropower and salmonids: Potential
623 effects and perspective on future research. *Canadian Journal of Fisheries and Aquatic Sciences*, *74*(7),
624 1135–1149. https://doi.org/10.1139/cjfas-2016-0253

625 Goffin, L., Dewals, B., Erpicum, S., Pirotton, M., & Archambeau, P. (2020). An Optimized and Scalable
626 Algorithm for the Fast Convergence of Steady 1-D Open-Channel Flows. *Water*, *12*(11), Article 11.
627 https://doi.org/10.3390/w12113218

628 Gore, J. A., & Banning, J. (2017). Chapter 3—Discharge Measurements and Streamflow Analysis. In F.
629 R. Hauer & G. A. Lamberti (Eds.), *Methods in Stream Ecology, Volume 1 (Third Edition)* (pp. 49–70).
630 Academic Press. https://doi.org/10.1016/B978-0-12-416558-8.00003-2

631 Harvey, A. C., Glover, K. A., Wennevik, V., & Skaala, Ø. (2020). Atlantic salmon and sea trout display
632 synchronised smolt migration relative to linked environmental cues. *Scientific Reports*, *10*(1), 3529.
633 https://doi.org/10.1038/s41598-020-60588-0

634 Havn, T. B., Thorstad, E. B., Teichert, M. A. K., Sæther, S. A., Heermann, L., Hedger, R. D., Tambets, M.,
635 Diserud, O. H., Borcherding, J., & Økland, F. (2018). Hydropower-related mortality and behaviour of
636 Atlantic salmon smolts in the River Sieg, a German tributary to the Rhine. *Hydrobiologia*, *805*(1), 273–
637 290. https://doi.org/10.1007/s10750-017-3311-3

638 Honkanen, H. M., Orrell, D. L., Newton, M., McKelvey, S., Stephen, A., Duguid, R. A., & Adams, C. E.
639 (2021). The downstream migration success of Atlantic salmon (*Salmo salar*) smolts through natural
640 and impounded standing waters. *Ecological Engineering*, *161*, 106161.
641 https://doi.org/10.1016/j.ecoleng.2021.106161

642 Hvidsten, N., Jensen, A., Vivås, H., Bakke, Ø., & Heggberget, T. (1995). Downstream migration of
643 Atlantic salmon smolts in relation to water flow, water temperature, moon phase and social
644 behaviour. *Nordic Journal of Freshwater Research*, *70*, 38–48.

645 Ibbotson, A. T., Beaumont, W. R. C., Pinder, A., Welton, S., & Ladle, M. (2006). Diel migration patterns
646 of Atlantic salmon smolts with particular reference to the absence of crepuscular migration. *Ecology*
647 *of Freshwater Fish*, *15*(4), 544–551. https://doi.org/10.1111/j.1600-0633.2006.00194.x

648 Jonsson, B., Jonsson, N., & Hansen, L. P. (1991). Differences in life history and migratory behaviour
649 between wild and hatchery-reared Atlantic salmon in nature. *Aquaculture*, *98*(1), 69–78.
650 https://doi.org/10.1016/0044-8486(91)90372-E

651 Jutila, E., & Jokikokko, E. (2008). Seasonal differences in smolt traits and post-smolt survival of wild
652 Atlantic salmon, Salmo salar, migrating from a northern boreal river. *Fisheries Management and*
653 *Ecology*, *15*(1), 1–9. https://doi.org/10.1111/j.1365-2400.2007.00562.x

654 Kobyshev, A., Bertrand, H., Randolf, I., Vandenberg, J., Stopa, K., Matthias, & Yasirroni, M. (2017).
655 *Suntime* (Version 1.3.2) [Computer software]. https://github.com/SatAgro/suntime

656 Lerquet, M., Colson, D., Beguin, J., & Sonny, D. (2021). *Rapport de suivi télémétrique des smolts de*
657 *saumon atlantique durant la phase de test pilote de mesures de protection sur les sites*
658 *hydroélectriques de Luminus* (Milestone No. 2; p. 38). https://www.life4fish.be/en/deliverables-and-
659 publications

660 Life4Fish. (2023). *Life4Fish*. https://www.life4fish.be/en

661 Lilly, J., Honkanen, H. M., McCallum, J. M., Newton, M., Bailey, D. M., & Adams, C. E. (2022).
662 Combining acoustic telemetry with a mechanistic model to investigate characteristics unique to
663 successful Atlantic salmon smolt migrants through a standing body of water. *Environmental Biology of*
664 *Fishes*, *105*(12), 2045–2063. https://doi.org/10.1007/s10641-021-01172-x

665 Lucas-Borja, M. E., Piton, G., Yu, Y., Castillo, C., & Antonio Zema, D. (2021). Check dams worldwide:
666 Objectives, functions, effectiveness and undesired effects. *CATENA*, *204*, 105390.
667 https://doi.org/10.1016/j.catena.2021.105390

668 Martin, P., Rancon, J., Segura, G., Laffont, J., Boeuf, G., & Dufour, S. (2012). Experimental study of the
669 influence of photoperiod and temperature on the swimming behaviour of hatchery-reared Atlantic
670 salmon (*Salmo salar* L.) smolts. *Aquaculture*, *362–363*, 200–208.
671 https://doi.org/10.1016/j.aquaculture.2011.11.047

672 Nilsen, C. I., Vollset, K. W., Velle, G., Barlaup, B. T., Normann, E. S., Stöger, E., & Lennox, R. J. (2023).
673 Atlantic salmon of wild and hatchery origin have different migration patterns. *Canadian Journal of*
674 *Fisheries and Aquatic Sciences*, *80*(4), 690–699. https://doi.org/10.1139/cjfas-2022-0120

675 Otero, J., L'Abée-Lund, J. H., Castro-Santos, T., Leonardsson, K., Storvik, G. O., Jonsson, B., Dempson,
676 B., Russell, I. C., Jensen, A. J., Baglinière, J.-L., Dionne, M., Armstrong, J. D., Romakkaniemi, A., Letcher,
677 B. H., Kocik, J. F., Erkinaro, J., Poole, R., Rogan, G., Lundqvist, H., … Vøllestad, L. A. (2014). Basin-scale
678 phenology and effects of climate variability on global timing of initial seaward migration of Atlantic
679 salmon (Salmo salar). *Global Change Biology*, *20*(1), 61–75. https://doi.org/10.1111/gcb.12363

680 Ovidio, M., Renardy, S., Dierckx, A., Nzau Matondo, B., & Benitez, J.-P. (2021). Improving bypass
681 performance and passage success of Atlantic salmon smolts at an old fish-hostile hydroelectric power
682 station: A challenging task. *Ecological Engineering*, *160*, 106148.
683 https://doi.org/10.1016/j.ecoleng.2021.106148

684 Peirson, W. L., & Harris, J. H. (2025). Potential for tube fishways to pass salmon upstream over high
685 dams. *Journal of Hydro-Environment Research*, *58*, 36–49. https://doi.org/10.1016/j.jher.2024.12.001

686 Philippart, J. C., Micha, J. C., Baras, E., Prignon, C., Gillet, A., & Joris, S. (1994). *The Belgian Project*
687 *"Meuse Salmon 2000". First Results, Problems and Future Prospects*. *29*(3), 315–317.
688 https://www.proquest.com/docview/1943292921/abstract/5075B9E4F3DA4E1DPQ/1

689 Philippart, J.-C. (2008). Les Poissons de la Vesdre. *Tribune de l'Eau*, *60*(643–644).
690 https://orbi.uliege.be/handle/2268/241408

691 Pompeu, C. R., Peñas, F. J., Goldenberg-Vilar, A., Álvarez-Cabria, M., & Barquín, J. (2022). Assessing
692 the effects of irrigation and hydropower dams on river communities using taxonomic and multiple
693 trait-based approaches. *Ecological Indicators*, *145*, 109662.
694 https://doi.org/10.1016/j.ecolind.2022.109662

695 Prignon, C., Micha, J. C., Rimbaud, G., & Philippart, J. C. (1999). Rehabilitation efforts for Atlantic
696 salmon in the Meuse basin area: Synthesis 1983–1998. *Hydrobiologia*, *410*(0), 69–77.
697 https://doi.org/10.1023/A:1003739327687

698 R Core Team. (2023). *The R Project for Statistical Computing* (Version 4.3.1) [Windows]. R Core Team.
699 https://www.r-project.org/

700 Renardy, S., Ciraane, U. D., Benitez, J.-P., Dierckx, A., Archambeau, P., Pirotton, M., Erpicum, S., &
701 Ovidio, M. (2023a). Combining fine-scale telemetry and hydraulic numerical modelling to understand
702 the behavioural tactics and the migration route choice of smolts at a complex hydropower plant.
703 *Hydrobiologia*, *850*(14), 3091–3111. https://doi.org/10.1007/s10750-023-05237-z

704 Renardy, S., Ciraane, U. D., Benitez, J.-P., Dierckx, A., Archambeau, P., Pirotton, M., Erpicum, S., &
705 Ovidio, M. (2023b). Combining fine-scale telemetry and hydraulic numerical modelling to understand
706 the behavioural tactics and the migration route choice of smolts at a complex hydropower plant.
707 *Hydrobiologia*, *850*, 3091–3111. https://doi.org/10.1007/s10750-023-05237-z

Renardy, S., Ciraane, U. D., Benitez, J.-P., Dierckx, A., Gelder, J., Silva, A. T., Archambeau, P., Dewals, B., Pirotton, M., Erpicum, S., & Ovidio, M. (2023). Assessment of the Attractiveness and Passage Efficiency of Different Fish Passage Solutions at a Hydropower Plant by Combining Fine Scale 2D-Telemetry and Hydraulic Numerical Modelling. *Environments*, *10*(7), Article 7. https://doi.org/10.3390/environments10070107

Renardy, S., Takriet, A., Benitez, J.-P., Dierckx, A., Baeyens, R., Coeck, J., Pauwels, I. S., Mouton, A., Archambeau, P., Dewals, B., Pirotton, M., Erpicum, S., & Ovidio, M. (2021). Trying to choose the less bad route: Individual migratory behaviour of Atlantic salmon smolts (Salmo salar L.) approaching a bifurcation between a hydropower station and a navigation canal. *Ecological Engineering*, *169*, 106304. https://doi.org/10.1016/j.ecoleng.2021.106304

Riley, W. D., Bendall, B., Ives, M. J., Edmonds, N. J., & Maxwell, D. L. (2012). Street lighting disrupts the diel migratory pattern of wild Atlantic salmon, *Salmo salar* L., smolts leaving their natal stream. *Aquaculture*, *330–333*, 74–81. https://doi.org/10.1016/j.aquaculture.2011.12.009

Roberts, L. J., Taylor, J., Gough, P. J., Forman, D. W., & De LEANIZ, C. G. (2009). Night stocking facilitates nocturnal migration of hatchery-reared Atlantic salmon, Salmo salar, smolts. *Fisheries Management and Ecology*, *16*(1), 10–13. https://doi.org/10.1111/j.1365-2400.2008.00611.x

Roy, R., Beguin, J., Watthez, Q., Goffaux, D., & Sonny, D. (2017). *Suivi des smolts de saumon en migration au niveau du tronçon de la Meuse exploité par 6 centrales hydroélectriques* (Synthesis No. 1; p. 79). PROFISH. https://www.life4fish.be/en/deliverables-and-publications

Scruton, D. A., McKinley, R. S., Kouwen, N., Eddy, W., & Booth, R. K. (2003). Improvement and optimization of fish guidance efficiency (FGE) at a behavioural fish protection system for downstream migrating Atlantic salmon (Salmo salar) smolts. *River Research and Applications*, *19*(5–6), 605–617. https://doi.org/10.1002/rra.735

731 Silva, A. T., Bærum, K. M., Hedger, R. D., Baktoft, H., Fjeldstad, H.-P., Gjelland, K. Ø., Økland, F., &
732 Forseth, T. (2020). The effects of hydrodynamics on the three-dimensional downstream migratory
733 movement of Atlantic salmon. *Science of The Total Environment*, *705*, 135773.
734 https://doi.org/10.1016/j.scitotenv.2019.135773

735 Silva, A. T., Lucas, M. C., Castro-Santos, T., Katopodis, C., Baumgartner, L. J., Thiem, J. D., Aarestrup, K.,
736 Pompeu, P. S., O'Brien, G. C., Braun, D. C., Burnett, N. J., Zhu, D. Z., Fjeldstad, H., Forseth, T.,
737 Rajaratnam, N., Williams, J. G., & Cooke, S. J. (2018). The future of fish passage science, engineering,
738 and practice. *Fish and Fisheries*, *19*(2), 340–362. https://doi.org/10.1111/faf.12258

739 Simmons, O. M., Gregory, S. D., Gillingham, P. K., Riley, W. D., Scott, L. J., & Britton, J. R. (2021).
740 Biological and environmental influences on the migration phenology of Atlantic salmon Salmo salar
741 smolts in a chalk stream in southern England. *Freshwater Biology*, *66*(8), 1581–1594.
742 https://doi.org/10.1111/fwb.13776

743 Sortland, L. K., Aarestrup, K., & Birnie-Gauvin, K. (2024). Comparing the migration behavior and
744 survival of Atlantic salmon () and brown trout () smolts. *Journal of Fish Biology*, *n/a*(n/a), 1–17.
745 https://doi.org/10.1111/jfb.15749

746 SPW, S. P. de W. (2024). *L'hydrométrie en Wallonie*. L'hydrométrie en Wallonie.
747 https://hydrometrie.wallonie.be/home.html

748 Strople, L. C., Filgueira, R., Hatcher, B. G., Denny, S., Bordeleau, X., Whoriskey, F. G., & Crossin, G. T.
749 (2018). The effect of environmental conditions on Atlantic salmon smolts' (Salmo salar) bioenergetic
750 requirements and migration through an inland sea. *Environmental Biology of Fishes*, *101*(10), 1467–
751 1482. https://doi.org/10.1007/s10641-018-0792-5

752 Szabo-Meszaros, M., Forseth, T., Baktoft, H., Fjeldstad, H.-P., Silva, A. T., Gjelland, K. Ø., Økland, F.,
753 Uglem, I., & Alfredsen, K. (2019). Modelling mitigation measures for smolt migration at dammed river
754 sections. *Ecohydrology*, *12*(7), e2131. https://doi.org/10.1002/eco.2131

Teichert, N., Benitez, J.-P., Dierckx, A., Tétard, S., de Oliveira, E., Trancart, T., Feunteun, E., & Ovidio, M. (2020). Development of an accurate model to predict the phenology of Atlantic salmon smolt spring migration. *Aquatic Conservation: Marine and Freshwater Ecosystems*, *30*(8), 1552–1565. https://doi.org/10.1002/aqc.3382

Thorstad, E. B., Bliss, D., Breau, C., Damon-Randall, K., Sundt-Hansen, L. E., Hatfield, E. M. C., Horsburgh, G., Hansen, H., Maoiléidigh, N. Ó., Sheehan, T., & Sutton, S. G. (2021). Atlantic salmon in a rapidly changing environment—Facing the challenges of reduced marine survival and climate change. *Aquatic Conservation: Marine and Freshwater Ecosystems*, *31*(9), 2654–2665. https://doi.org/10.1002/aqc.3624

Thorstad, E. B., Whoriskey, F., Uglem, I., Moore, A., Rikardsen, A. H., & Finstad, B. (2012). A critical life stage of the Atlantic salmon Salmo salar: Behaviour and survival during the smolt and initial post-smolt migration. *Journal of Fish Biology*, *81*(2), 500–542. https://doi.org/10.1111/j.1095-8649.2012.03370.x

Tortajada, C. (2015). Dams: An Essential Component of Development. *Journal of Hydrologic Engineering*, *20*(1), A4014005. https://doi.org/10.1061/(ASCE)HE.1943-5584.0000919

Van Rijssel, J. C., Breukelaar, A. W., De Leeuw, J. J., Van Puijenbroek, M. E. B., Schilder, K., Schrimpf, A., Vriese, F. T., & Winter, H. V. (2024). Reintroducing Atlantic salmon in the river Rhine for decades: Why did it not result in the return of a viable population? *River Research and Applications*, *40*(7), 1164–1182. https://doi.org/10.1002/rra.4284

Van Rossum, G., & Drake Jr, F. L. (1995). *Python 3* (Version 3) [Computer software]. https://www.python.org/downloads/release/python-31011/

Vollset, K. W., Lennox, R. J., Lamberg, A., Skaala, Ø., Sandvik, A. D., Sægrov, H., Kvingedal, E., Kristensen, T., Jensen, A. J., Haraldstad, T., Barlaup, B. T., & Ugedal, O. (2021). Predicting the

778 nationwide outmigration timing of Atlantic salmon (Salmo salar) smolts along 12 degrees of latitude
779 in Norway. *Diversity and Distributions*, *27*(8), 1383–1392. https://doi.org/10.1111/ddi.13285

780 Wang, X., Chen, Y., Yuan, Q., Xing, X., Hu, B., Gan, J., Zheng, Y., & Liu, Y. (2022). Effect of river damming
781 on nutrient transport and transformation and its countermeasures. *Frontiers in Marine Science*, *9*.
782 https://doi.org/10.3389/fmars.2022.1078216

783 Watson, S., Schneider, A., Santen, L., Deters, K. A., Mueller, R., Pflugrath, B., Stephenson, J., & Deng, Z.
784 D. (2022). Safe passage of American Eels through a novel hydropower turbine. *Transactions of the*
785 *American Fisheries Society*, *151*(6), 711–724. https://doi.org/10.1002/tafs.10385

786 Whalen, K. G., Parrish, D. L., & McCormick, S. D. (1999). Migration Timing of Atlantic Salmon Smolts
787 Relative to Environmental and Physiological Factors. *Transactions of the American Fisheries Society*,
788 *128*(2), 289–301. https://doi.org/10.1577/1548-8659(1999)128<0289:MTOASS>2.0.CO;2

789 Zydlewski, G. B., Stich, D. S., & McCormick, S. D. (2014). Photoperiod control of downstream
790 movements of Atlantic salmon Salmo salar smolts. *Journal of Fish Biology*, *85*(4), 1023–1041.
791 https://doi.org/10.1111/jfb.12509

792